

## APPLICATION OF SINMAP AND ANALYSIS OF MODEL SENSITIVITY – CASE STUDIES FROM GERMANY AND CHINA

BENNI THIEBES\*, RAINER BELL\*\*, THOMAS GLADE\*\*\*,  
JIAN WANG\*\*\*\*, SHIBIAO BAI\*\*\*\*\*

*Key-words:* landslides; SINMAP; susceptibility mapping; sensitivity analysis.

**Abstract.** Landslides cause significant damage in many parts of the world and consequently many efforts have been made to forecast the spatial probability of future slope failures. In particular regional landslide susceptibility and hazard models have become popular over the last years because they delineate areas which are likely to experience slope failures in the future, which is important, e.g. for spatial planning purposes. In this study, the physically-based model SINMAP (Stability Index Mapping) was applied to two study areas with different geo-environmental conditions; one in the Swabian Alb, Germany, and one in Youfang catchment, Wudu county, Western China. A sensitivity analysis of the geotechnical input parameters was carried out to determine their influence on model outputs. The results show that the majority of observed landslides are located within areas that have been classified as likely to experience slope failure. The spatial resolution of input data has an effect on SINMAP results, however, the difference between 10 m and 30 m data was found to be relatively small. Sensitivity analysis revealed that internal friction has a large influence on susceptibility modelling, while the hydrological parameter  $T/R$  only changed the results to a very small extent under the parameter range tested in this study. Based on the results it can be concluded that SINMAP is capable of appropriately computing regional landslide susceptibility for large areas and can provide useful information, especially when high detail topography data is available. The results of sensitivity analysis can be expected to be helpful for other researchers for a more successful application of SINMAP to other study areas.

### 1. INTRODUCTION

Landslides are natural phenomena occurring in many parts of the world and their damage potential is often underestimated. A recent study by Petley (2012) concluded that between 2004 and 2010 32,322 lives were lost due to non-seismic-triggered landslide events, relating to an average annual death toll of approximately 4,617. In addition to fatalities due to catastrophic slope failures, landslides cause significant direct and indirect damage, for example due to destruction of infrastructure, blockages of roads and interruption of life-lines, as well as the degradation of agricultural land. For China, Yin (2009) estimated direct annual economic losses of approximately 10 billion RMB (approximately US-\$ 1.65 billion) and 900 fatalities. Even in Germany with its relatively low fraction of high mountain areas, the annual damage has been calculated to be US-\$ 150 million (Krauter, 1992).

---

\* Senior researcher, Institute for Applied Remote Sensing, European Academy Bozen/Bolzano (EURAC), Italy, Viale Druso 1, 39100 Bolzano, Italy; benni.thiebes@eurac.edu; benni.thiebes@gmail.com.

\*\* Senior Researcher, Department of Geography and Regional Research, University of Vienna, Universitätsstr. 7, 1010 Vienna, Austria, rainer.bell@univie.ac.at.

\*\*\* Professor, Department of Geography and Regional Research, University of Vienna, Universitätsstr. 7, 1010 Vienna, Austria, thomas.glade@univie.ac.at.

\*\*\*\* Professor, School of Geography Science and Key Laboratory of Virtual Geographical Environment, Nanjing Normal University, no. 1 Wenyuan Road, Nanjing 210046, P.R. China, jwang@njnu.edu.cn.

\*\*\*\*\* Associate Professor, School of Geography Science and Key Laboratory of Virtual Geographical Environment, Nanjing Normal University, no. 1 Wenyuan Road, Nanjing 210046, P.R. China, shibiaobai@njnu.edu.cn.

Fostered by the advances in computer technology and in particular the advent of Geographic Information Systems (GIS) in the 1990s, an increasing number of regional landslide susceptibility, hazard and risk maps were prepared to aid spatial planning and to avoid the consequences of slope failures (e.g. Catani *et al.*, 2005; Guzzetti *et al.*, 2005; Bell, 2007; Cascini, 2008; Chung, 2008; Fell *et al.*, 2008; Bai *et al.*, 2009; Bai *et al.*, 2010c). Regional methodologies can broadly be grouped into heuristic, inventory-based, statistical and deterministic approaches (Soeters, Van Westen, 1996; Aleotti, Chowdhury, 1999; Guzzetti, 1999; Van Westen *et al.*, 2006). Deterministic models are based on the laws of physics and generally apply simulations of water flow on slopes and a calculation of slope stability with geotechnical equations. The most frequently applied regional deterministic models are one-dimensional, such as the infinite slope stability model (Hammond *et al.*, 1992; Montgomery, Dietrich, 1994; Wu, Sidle, 1995, 1997; Sidle, Wu, 1999). These approaches are based on the concept of topographically induced wetness initially proposed by Beven and Kirkby (1979). The simplicity of the infinite slope model makes it possible to compute slope stability in GIS.

One such model is SINMAP (Stability Index Mapping), which allows for a relatively quick analysis of landslide susceptibility over large areas even with limited data availability (Pack *et al.*, 1998, 2001, 2005). SINMAP has been successfully applied by many landslide researchers and practitioners, and the majority reported satisfying modelling results with high proportions of known landslides being located in the areas modelled as most susceptible (Morrissey *et al.*, 2001; Zaitchik *et al.*, 2003; Zaitchik, Van Es, 2003; Meisina, Scarabelli, 2007; Thiebes *et al.*, 2007; Weerasinghe *et al.*, 2007). Some authors reported over-prediction of landslide susceptibility (Morrissey *et al.*, 2001; Meisina, Scarabelli, 2007). A number of researchers chose to combine SINMAP simulations with additional analyses, including statistical methods (Zaitchik *et al.*, 2003), calculations of certainty factors (Lan *et al.*, 2004) and the application of the most likely landslide initiation point method (MLIP) (Tarolli, Tarboton, 2006). Legorreta Paulin *et al.* (2010) compared SINMAP to a multiple logistic regression model and found that SINMAP was less affected by pixel resolution, with relatively constant results for 1 m, 5m, and 10 m pixels. However, with 30 m pixels, SINMAP predictions were inefficient for small and shallow landslides. Comparisons of SINMAP with similar deterministic slope stability models have been presented by Meisina and Scarabelli (2007) for SHALSTAB, and Morrissey *et al.* (2001) for LISA and Iverson's Transient Response Model. The majority of SINMAP applications concentrated on shallow translational slides; however, in some works other processes such as debris flows (Morrissey *et al.*, 2001) and deep-seated landslides (Kreja, Terhorst 2005, 2009; Legorreta Paulin *et al.* 2010) have been included. Despite the large number of published SINMAP studies, no complete sensitivity analysis of all involved parameters has been reported yet. However, such information would be highly desirable for future SINMAP applications to be able to focus investigations on the most effective parameters and to achieve more reliable modelling results. Moreover, some of the results of partial sensitivity analyses contradict each other; Zaitchik *et al.* (2003) reported a relative low sensitivity to the cohesion factor and to soil thickness, but a high sensitivity to internal frictions and transmissivity. In contrast, Meisina and Scarabelli (2007) detected a strong influence of cohesion factor on modelling results, and Morrissey *et al.* (2001) described rainfall as one of the most influential factors.

In this paper, the application of the physically-based landslide model SINMAP to two study areas with different geo-environmental conditions is presented. The first study area is located in the Swabian Alb in south-west Germany, the second in the Youfang catchment, Wudu region in China's western Province Gansu. SINMAP was applied to both study sites in order to assess the regional landslide susceptibility and to evaluate the ability of the model for the delineation of spatial landslide probability. Besides the comparison of modelling results between the two study areas, a sensitivity analysis of the involved geotechnical parameters was carried out which has not been described in the literature yet.

## 2. STUDY AREAS

### 2.1. Swabian Alb

The first study area of this research is located in the Swabian Alb, a mountain range in southwest Germany (Fig. 1). The lithology of the Swabian Alb consists primarily of Jurassic clay underlying marl and limestone strata, of which the latter form a steep escarpment which stretches in a southwest-northeast direction for some 200 km. Elevations reach up to 1,000 m.a.s.l. in the western part, and range between 600 and 800 m.a.s.l. in the central and eastern sections, respectively. Landslides are a common geomorphological feature in the region due to lithological conditions (Terhorst, 1997) and triggering impact of rainfall events, snow melting and earthquakes (Meyenfeld, 2009). In total, approximately 30,000 landslide bodies of various sizes and ages can be assumed for the entire Swabian Alb (Bell, 2007). The most recent large landslide event was the Mössingen rockslide that took place in 1983. During this event, approximately 6 million cubic meters of material were triggered by exceptionally wet conditions (Fundinger, 1985; Bibus, 1986; Schädel, Stober, 1988). Several authors emphasise the importance of landslides for the relocation of the cuesta escarpment and the evolution to the present landscape (Bleich, 1960; Terhorst, 1997; Bibus, 1999), but landslides also represent a significant geo-hazard at present (Kallinich, 1999; Kreja, Terhorst, 2005; Bell, 2007; Neuhäuser, Terhorst, 2007; Papathoma-Köhle *et al.*, 2007; Terhorst, Kreja, 2009; Thiebes, 2012).

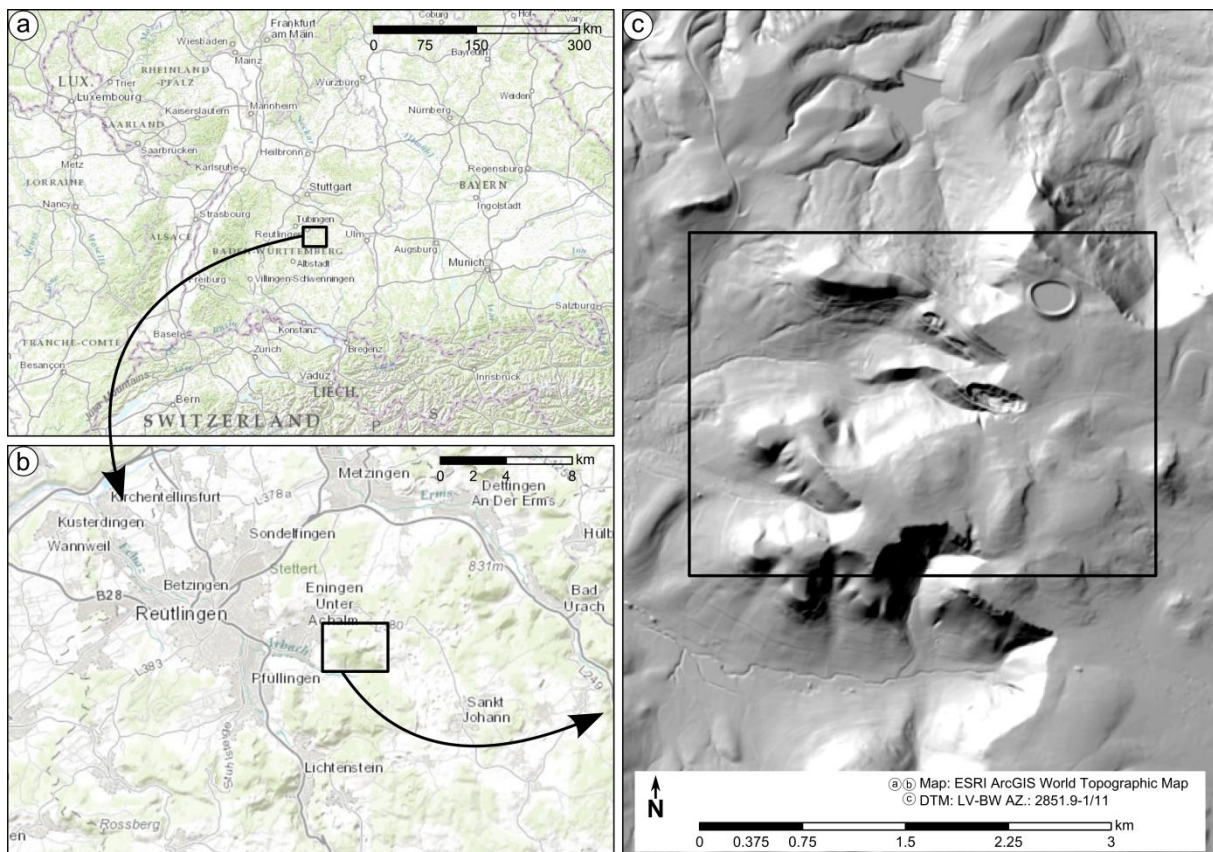


Fig. 1 – The study area Eningen in the Swabian Alb. Please note that the circular shape in the north-eastern corner of the study area is a reservoir of a hydro-electricity plant.

The main study area, for which susceptibility mapping was carried out, covers 8.5 km<sup>2</sup> and is located in Eningen, a small town east of Reutlingen. Elevations in the study area range between 500 m and 750 m a.m.s.l. The lithology includes Upper Jurassic limestone and marl strata which are slightly dipped into a south-west direction by 1 – 2° (Leser, 1982). The slopes are mostly covered by debris with a depth of 2 – 6 m (Ohmert *et al.*, 1988), which derives from Pleistocene solifluction and activity of shallow landslides. The study area includes parts of the relatively flat plateau area, the steep escarpment built by limestone (*Albtrauf*), and lower slopes consisting of Middle Jurassic marls and clays. The steep slopes are covered by forests, while the lower slopes and the plateau are used as grass-and-farmland. The mean annual precipitation for the closest weather station is 942 mm, however, climatic conditions are strongly influenced by orographic effects. Given the small size of the study area Eningen, and the availability of highly detailed light detection and ranging (LiDAR) topography, landslide mapping was carried out by a desk-based study of the digital terrain model (DTM) and its derivatives (e.g. hillshades, slope map), as well as by field investigations in which the mapped landslides were validated and additional landslides were recorded. In total, 141 shallow landslides were mapped which add up to an area of 0.14 km<sup>2</sup>, or 1.7% of the study area. The majority of shallow landslides occur on steep slope segments and in topographic hollows. More than 70% of the landslides are smaller than 1,000 m<sup>2</sup>. These slope failures generally have a depth of less than 2 m and do not involve the bedrock. Larger landslides, in some cases covering more than 2,500 m<sup>2</sup> make up more than 70% of the landslide-affected areas in the study area. These slope failures are mostly complex landslides involving translational movements in the upper part and a flow-like run-out. In addition to the aforementioned slope failures, even larger mass movements are present in the study area. These are large rotational failures which transition into flow movements in the lower parts. However, these landslides were excluded from this study.

## 2.2. Youfang

The second study area is Youfang catchment located in Beiyuhe basin in Wudu county, Longnan prefecture, in southern Gansu Province, north-western China (Fig. 2). This region is surrounded by the Qinghai-Tibet Plateau to the West, the Loess Plateau to the North, and the Sichuan Basin to the South. Wudu region features steep slopes reaching maximum elevations of more than 3,500 m a.m.s.l. while valley floors are as low as 1,000 m a.m.s.l. The V-shaped valleys are deeply incised and accommodate fast-flowing rivers. The steep slopes of this rural region are often terraced and are used for agriculture. The lithology of the study area includes a variety of strata among which Devonian and Silurian phyllites, slates and schists, as well as loess deposits which are known for a high landslide susceptibility (Li 1997). The area features a high tectonic activity with frequent earthquakes due to the uplift of the Qinghai-Tibet plateau. The region has a semi-arid, monsoon-influenced climate with cold winters and hot and moderately humid summers. Mean annual rainfall is influenced by the orographic effects of the high mountains and totals between 400 mm and 900 mm (Chen *et al.*, 2006). Approximately 80% of the annual rainfall is recorded between May and September with maximum hourly and daily precipitation as high as 40 mm and 90 mm, respectively. The combination of steep topography, weak lithologic formations and the high activity of triggering events make Wudu region one of the most landslide-prone areas in China (Scheidegger, Ai, 1987), and consequently, several landslide-related investigations have been carried out (Chen, 2004; Bai *et al.*, 2009, 2010a, 2010b, 2012). Landslides represent an important geo-hazard in the region and significant damage has been reported. For example, a single rainfall event on August 3, 1984 triggered more than 400 debris flows and 570 landslides which affected approximately 9.3 million people and caused a direct economic loss of 265 million RMB (approximately US-\$ 42 million) (Chen *et al.*, 2006). In total, at least 567 people were killed by landslides in the past four decades (China Geological Survey Bureau of Statistics, 2008). The

most recent example of the catastrophic effects of landslides in Southern Gansu was a debris flow in Zhouqu which occurred on August 8, 2010. A localised rainfall event triggered this fast-moving debris flow which swept through the city and destroyed large areas claiming at least 1,287 lives (Yu *et al.*, 2010). Earthquakes are another important landslide triggering agent and over the past decades seismic-triggered landslides often blocked rivers by landslide dams (Chen, 2004). A recent study on the influence of environmental factors concluded that in particular lithology, aspect, elevation, and distance to rivers and to faults strongly influence the spatial distribution of landslide (Bai *et al.*, 2012). Moreover, the on-going urbanisation of the area, and the reconstruction works following the Wenchuan earthquake in 2008 have increased the impacts of landslide occurrences on society (Chen *et al.*, 2006).

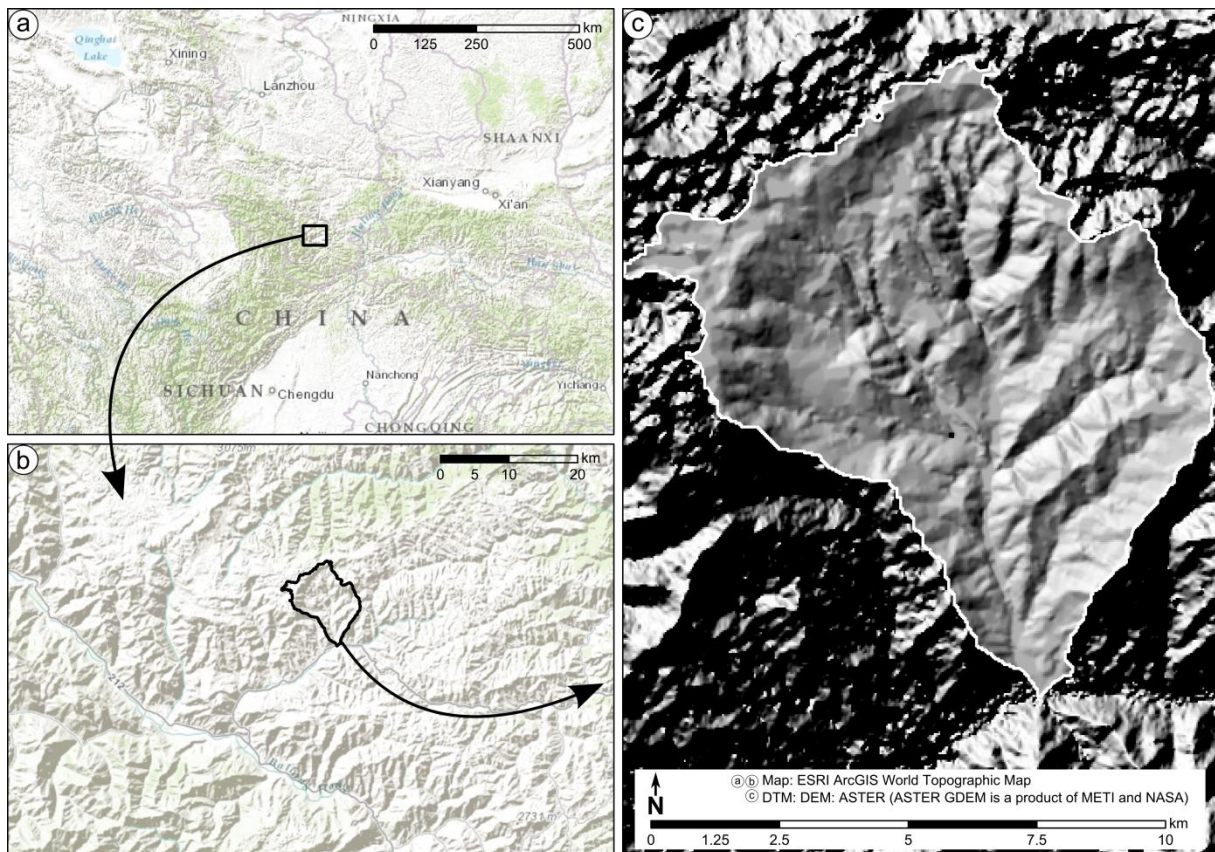


Fig. 2 – The study area Youfang catchment in southern Gansu Province.

The Chinese study area in which SINMAP was applied is Youfang catchment which covers 47.5 km<sup>2</sup> and is located approximately 15 km north-east of the provincial capital Longnan. Due to the size and remote location of the Youfang study area, as well as the non-availability of highly detailed topographic data, landslide mapping could not be carried out in the same way as for the German study area. Instead, a landslide inventory based on the interpretation of optical remote sensing data and provided by the Chinese Geological Survey in which rainfall-triggered landslides that occurred between 1995 and 2003 were recorded, was used. Field investigations and additional validation by optical remote sensing data revealed that the areas mapped as landslides rather cover landslide affected areas than single landslide bodies; several landslides as well as non-affected areas were combined within single polygons. Improvements of the available inventory proved to be extremely difficult since agricultural activities, in particular terracing, quickly lead to destruction of geomorphological evidence

of landslides. Consequently, the inventory was used in its original form. In total, 65 landslides were mapped which in total cover approximately 14% of the study area. The landslide inventory is classified according to the Chinese system and includes rock, colluvial and loess landslides. Within the international landslide classification by Cruden and Varnes (1996), the landslides can be defined complex slope failures including primarily translational and to a minor extent also rotational slides of regolith which in some cases exhibit a flow type run-out. The landslides in Youfang catchment developed within highly permeable materials such as colluvial slope debris of Pleistocene age, and loess deposits which are located above relatively impermeable bedrock. As Youfang catchment is heavily used for agriculture and terracing of slopes is very common practice, almost all landslides took place on slopes which have been significantly altered by human modification. Landslides in the study area are mostly located in topographic hollows, which hints the influence of water convergence on landslide initiation. The landslides greatly vary in size, with small landslides from a few hundred or thousand m<sup>2</sup> up to the largest; which according to the inventory; cover areas of up to 250,000 m<sup>2</sup>.

### 3. METHODS AND DATA

#### 3.1. SINMAP model

SINMAP is a physically-based software relying on the infinite slope stability model that is available free of cost as an extension to ESRI ArcView 3 and ArcGIS 9. The model was developed by Pack *et al.* (1998, 2001, 2005) to carry out regional susceptibility assessments of translational landslides in British Columbia. A brief introduction to SINMAP's theoretical background is provided below, more detailed explanations can be found in the technical handbooks (Pack *et al.*, 1998, 2005).

SINMAP couples the infinite slope stability model and a steady-state topographic hydrologic model. A basic assumption of the infinite slope model is that a permeable soil layer parallel to the ground surface overlies an impermeable layer such as bedrock. The contact zone between the layers is considered the shear surface for potential slope failures. Shallow subsurface water flow is simulated following the topographic gradient and deep drainage is neglected. Higher saturation develops in concave slope areas and reduces internal friction and cohesion which leads to decreased slope stability.

The basic stability calculation within SINMAP is described by

$$FoS = \frac{C + \cos\theta[1 - wr] \tan\phi}{\sin\theta} \quad (1)$$

where  $FoS$  is the Factor of Safety;  $C$  is the dimensionless cohesion value integrating both soil and root cohesion, as well as soil density and thickness;  $\theta$  is the slope angle;  $w$  is the relative wetness as the relation of water-table height to soil thickness;  $r$  is the constant soil density ratio;  $\phi$  is the internal friction angle. Relative wetness ( $w$ ) is modelled as induced by topographic conditions and depends on the specific catchment ( $a$ ) area of a given point (Tarboton, 1997), the effective water recharge  $I$  for a critical period of wet weather and the soil transmissivity ( $T$ ), i.e. hydraulic conductivity times soil thickness. In SINMAP,  $T/R$  is used as an input parameter rather than  $R/T$  because it can be interpreted as the length of a straight slope required to reach saturation. To define the stability of an area, the wetness index  $w$  is incorporated into the dimensionless Factor of Safety equation

$$FoS = \frac{C + \cos\theta[1 - \min(\frac{K}{T} \frac{a}{\sin\theta}, 1)r] \tan\phi}{\sin\theta} \quad (2)$$

The specific catchment area ( $a$ ) and the slope angle are derived from the DTM topography, while cohesion ( $C$ ), internal friction ( $\phi$ ) and the combined factor  $R/T$  are soil-hydrological parameters.

In SINMAP's slope stability calculation, parameter uncertainty for the last three parameters is incorporated and uniform probability distributions between given minimum and maximum values are assumed. Areas for which the worst case parameter constellations result in a *FoS* of greater than 1 are considered unconditionally stable. For all other areas, there is a probability of failure that is expressed as the Stability Index (*SI*). When even the best case parameter constellations result in a *FoS* of less than 1, a *SI* of 0 is assigned. These areas are considered unconditionally unstable (*defended*). In total, SINMAP differentiates six *SI* classes. *Stable*, *moderately-stable* and *quasi-stable* classes have a minimum *SI* greater than 1 and represent regions that should not fail with the most conservative parameters in the specified range. For these areas, external destabilising factors would be required to cause instability. For the *lower-and-upper-threshold* classes the calculated *SI* is smaller than 1, and the probability of failure is less than or greater than 50%, respectively. For *lower-threshold* areas, no external destabilising factors are required for instability; for *upper-threshold* areas stabilising factors might be responsible for stability.

### 3.2. Base data

SINMAP requires three essential types of input data to perform the stability calculation: topographic data as a grid-based DTM, maps displaying the spatial distribution of surface material (calibration areas), e.g. lithology, and their respective geotechnical properties, and an inventory of past landslide occurrences. An overview on the base data used in this study is presented in Table 1.

Table 1

Input data used within the study

Type	Comment	Resolution	Source
<b>Swabian Alb</b>			
DTM	Airborne LiDAR data	1 m x 1m	STATE OFFICE OF LAND SURVEY (LVBW)
Geological map	Map sheet 7,520 Reutlingen	1:50000	STATE OFFICE OF GEOLOGY, RESOURCES AND MINING (LGRB)
Land use map	Only forest was considered	1:25000	STATE OFFICE OF LAND SURVEY (LVBW)
Geotechnical parameters	Literature values	–	MEYENFELD (personal communication)
Landslide inventory	Mapping	Polygons	LiDAR and field mapping
<b>Youfang</b>			
DTM	Digitised from 1:50000 topographic map	30 m x 30 m	NATIONAL ADMINISTRATION OF SURVEYING, MAPPING AND GEOINFORMATION
Geological map	Lithological classes combined based on geomechanical characteristics	1:200000	CHINA GEOLOGICAL SURVEY; WU & WANG (2006)
Geotechnical parameters	Laboratory testing	–	WU & WANG (2006)
Landslide inventory	Mapping from optical remote sensing data	Polygons	CHINESE GEOLOGICAL SURVEY
LVBW = Landesvermessungsamt Baden-Württemberg; LGRB = Landesamt für Geologie, Rohstoffe und Bergbau Baden-Württemberg			

### 3.2.1. Swabian Alb

For the study area in the Swabian Alb, a LiDAR-based DTM with a 1m-scale was available. For the SINMAP simulations, the spatial scale was decreased to 10 m by the ArcGIS ‘resample’ function using the nearest neighbour algorithm. Another DTM with 30 m pixels was created to allow for an easier comparison of results to the study area in China. A geological map (1:50000) was used to describe the spatial distribution of surface materials. In this study, it was not possible to assess the geotechnical parameters for the respective lithological units by laboratory analyses, and instead a database of geotechnical values extracted from literature sources (Meyenfeld, personal communication) was used. The determination of the cohesion and friction angle values was relatively straightforward due to the availability of several laboratory tests with similar materials published in the literature. The soil-hydrological factor  $T/R$ , however, could not easily be assigned based on literature values because it is only used in SINMAP. Therefore, the default values of  $T/R$  (Pack *et al.*, 1998, 2001; Pack & Tarboton 2004; Pack *et al.*, 2005) were used and modified for the lithology classes in the study area: for clayey materials, the minimum  $T/R$  values were decreased for up to 1,000 units to meet the water retaining characteristics; for more permeable materials, the value was increased for up to 250 units. In addition, the calibration tool implemented in SINMAP (i.e. SA plots) was used to define more appropriate parameter values. Thereto, modelling is repeated using modified parameter values until a satisfactory proportion of landslides was computed in areas of low stability. To be able to carry out a comparable sensitivity analysis, the range between the lower and the upper bounds of the geotechnical parameters for friction angle and  $T/R$  were chosen to be the same for all geotechnical classes. For friction angles, a difference of  $10^\circ$  was chosen, and for the hydrological parameter  $T/R$  a range of 1,000 units between minimum and maximum values was selected. Thereby, the selected ranges are the same as described in the SINMAP handbook. The stabilising influence of vegetation on slope stability was also included for the Swabian Alb case study. The spatial distribution of forests in the study area was extracted from a digital land-use map (1:25000) and merged with the geology map. For all areas covered with forest, the upper bound of cohesion was increased by  $10 \text{ KN/m}^2$ , which is similar to the values used in other studies (Hammond *et al.*, 1992; Sidle, Wu 1999; Sidle, Wu 1999). Given the fact that the determination of geotechnical parameters involved significant subjective input, the chosen values were subsequently calibrated by repeated SINMAP simulations and an analysis of the results. The landslide inventory derived from desk- and field-based analyses was converted to a raster data-set with a spatial resolution equivalent to the DTM using the ‘maximum area function’ of the ArcGIS ‘polygon to raster’ tool: each pixel of the raster map is assigned the value of the feature (landslide or non-landslide) that fills the greater part of that specific pixel. Thereby, the rasterised landslide map can exclude areas within the original landslide boundaries, or include areas formerly outside the boundary.

### 3.2.2. Youfang

For the study area in Youfang catchment, a 1:50000 topographic map was available; the contour lines were digitised and transformed to DTM with 30 m grid resolution using the ‘Topo to raster’ function in ArcGIS. Information on the spatial distribution of surface materials was available in the form of a geological map (1:200,000) produced by the China Geological Survey. Unfortunately larger-scale maps of the study area are not available for research purposes. It is important to note that the Geological map does not describe any loess in the study area even though field evidence confirms the presence of loess deposits. The aforementioned map had been aggregated by Wu and Wang (2006) based on the geomechanical characteristics of the respective lithological classes. For the displayed units, the geotechnical parameters cohesion and friction angle were determined from the values provided by Wu and Wang (2006), who carried out laboratory tests of material properties in a study area close to Youfang catchment. The  $T/R$  values were assigned in the same way as in the German

study area, i.e. by modifications of the default values by subjective interpretation, as well as calibration, using the SINMAP SA plots. No information on vegetation cover was readily available and consequently the strengthening effect of root cohesion was not taken into account. The landslide inventory provided by the Chinese Geological Survey in which the boundaries of landslide-affected areas were mapped was transferred to a raster map in the same way as for the German study area.

### 3.3. Application of SINMAP

In this study, the SINMAP version developed for ArcView 3 was used to run the model because the newer version for ArcGIS 9 produced error messages. According to one of the SINMAP developers, this is caused by some bugs related to the conversion of SINMAP from ArcView 3 into ArcGIS 9 (Tarboton, personal communication). The results of the SINMAP simulations, i.e. the stability index maps, were exported and analysed in ArcGIS 9. Parameter settings were calibrated by repeated simulation runs with slightly different parameter settings, as well as by using the in-build calibration tools (SA plots). The resulting maps were evaluated based on their agreement with the spatial landslide distributions (proportion of landslides captured within highly susceptible areas), as well as their geomorphological quality. Quality assessment of a SINMAP simulation traditionally uses point data describing landslide locations. However, in this study landslide data were available as polygon data describing the entire spatial extent of slope failures. Therefore, it was decided to include the entire landslide-affected area for the assessment of SINMAP modelling results. The ‘raster calculator’ tool in ArcGIS was used to create grids in which only the landslide-affected stability classes are displayed which then could be used for a statistical analysis. *No data* areas are primarily caused by the hydrological simulations by SINMAP; for each cell of the DTM the flow direction and the specific catchment area is calculated. Cells for which no specific catchment area can be calculated, e.g. the uppermost cells, are assigned the *no data* value.

### 3.4. Sensitivity analysis

A sensitivity analysis of the model input parameters cohesion, internal friction and the hydro-geological parameter  $T/R$  was carried out to assess their influence on SINMAP slope stability calculation. The initially determined minimum and maximum values assigned to the lithological classes, referred to the following as ‘standard values’, were manually modified in 10%-steps in the range between 50% and 150% of the standard values. This range was selected because it was considered to cover the realistic possible range of the real parameter values. During the sensitivity analyses, only one parameter’s minimum and maximum values were adjusted at a time, while all the other parameters were kept at their original value. Then, the model simulation was repeated and the resulting maps were analysed for the distribution of the stability classes. For cohesion, this procedure was not possible because the standard value for the minimum cohesion was set to zero to allow for completely saturated conditions in which no soil cohesion is present. Therefore, only the upper bound of cohesion ( $C_{max}$ ) was treated in the same way as described above, and the lower cohesion bound ( $C_{min}$ ) remained zero. In a last step all parameters except for  $C_{min}$  were kept at their standard values and only  $C_{min}$  was raised to the standard value of  $C_{max}$  (100% scenario) and then gradually decreased in 10% steps to its original value (0% scenario). The sensitivity analysis was carried out with 10m-and-30m-scale for the study area in the Swabian Alb, and with 30 m data for the study area in Youfang.

## 4. RESULTS

### 4.1. Input data

#### 4.1.1. Swabian Alb

The geological map scaled 1:50000 displays a total of 20 classes from Middle and Upper Jurassic, and the Quaternary and Tertiary. Table 2 lists the classes and their geotechnical parameter values for the standard scenarios (100% parameter values). The combination with the forest distribution from the land-use map (1:25000), the combination of classes with the same geotechnical parameter values and the aggregation of classes with only small spatial extents during the following conversion to a 10 m raster resulted in a total of 23 classes based on lithology and vegetation. The change of spatial resolution to 30 m reduced the total number of classes to 14. In addition, the representation of the topography changed with an altered pixel resolution; steep areas occur less often and small topographic hollows, important for flow convergence, are often levelled out. Additional effects could be observed for the landslide inventory; the areas affected by landslides slightly decreased from the original inventory to the 1 m and the 30 m DTM.

Table 2

Geotechnical parameter values for the classes of the Geological map (1:50000) for the Swabian Alb. Descriptions are based on Ohmert *et al.*, 1988; Geyer, Gwinner, 1986; Wagenplast, 2005; and Bell, 2007

	Class	Description	$C_{min}$	$C_{max}$	$\Phi_{min}$	$\Phi_{max}$	$T/R_{min}$	$T/R_{max}$
Quaternary and Tertiary	Floodplain sediments	–	0	0.3	20	30	1,500	2,500
	Calcerous sinter	–	0	0.2	25	35	2,250	3,250
	Loess sediments	–	0	0.3	20	30	1,750	2,750
	Colluvium	–	0	0.25	20	30	2,000	3,000
	Slope debris	solifluction and landslide activity	0	0.15	25	35	2,000	3,000
	Basalt tuff	volcanic activity in Miocene	0	0.15	15	25	2,000	3,000
	Xenolith in basalt tuff		0	0.15	15	25	2,000	3,000
Upper Jurassic	Zementmergel (ki5)	lime marls, marl lime and lime; partly massive	0	0.25	20	30	1,750	2,750
	Liegender Bankkalk (ki4)	alternating sequences of lime- and-marl lime separated by marl beds	0	0.2	25	35	2,250	3,250
	Unterer Massenkalk (joMu)	massive and compact limestone	0	0.2	20	30	2,250	3,250
	Unterer Massenkalk und Zuckerkorn-Dolomit Fazies (joMuZD)	cavernous dolomite limestones	0	0.2	20	30	2,250	3,250
	Unterer Felsenkalk (ki2)	dominantly massive lime; partly layered limestone beds	0	0.2	20	30	2,250	3,250
	Lacunosamergel (ki1)	marl limestone with varying clay content	0	0.25	20	35	1,750	2,750
	Wohlgeschichter Kalk (ox2)	uniformly stratified limestone with thin marl beds; partly massive	0	0.2	23	33	2,250	3,250
	Impressamergel (ox1)	alternation of marl and marl lime beds	0	0.25	20	35	1,750	2,750
Middle Jurassic	Ornatenton (cl)	clay stones with oolitic iron horizons	0	0.3	20	30	1,000	2,000
	Dentalienton (bt)	clay stones with interstratified marl lime beds	0	0.25	20	30	1,000	2,000
	Hamitenton (bj3)	dominantly clay stones	0	0.25	20	30	1,000	2,000
	Ostreenkalk (bj2)	plastic clays and clay marls, inter-stratified marl lime beds	0	0.25	25	30	1,750	2,750
	Blaukalk (BL)	marl and dolomite limestone	0	0.25	25	35	2,250	3,250

The assigned parameter values for  $C_{min}$  are 0 for all classes.  $C_{max}$  ranges between 0.15 KN/m<sup>2</sup> for unconsolidated slope debris and reaches a maximum of 0.3 KN/m<sup>2</sup> for the claystones of the *Ornatenton*. The lowest friction angles were assigned to the basalts for which the lower and upper bounds were set to 15° and 25°, respectively; the highest values are related to slope debris and *Blaukalk* for which the lower and upper bounds are 25° and 35°, respectively. Minimum values for  $T/R$  range from 1,000 for the clay rich materials of the Middle Jurassic, and the highest value of 2,250 was assigned to the limestone areas which are assumed to be influenced by karst processes.

#### 4.1.2. Youfang

The aggregated geological map for Youfang catchment displays three lithology units in the study area. These include phyllites, sand- and-mudstones, and limestones and slates (Table 3). With respect to the laboratory analyses by WU & WANG (2006), the lowest friction angle in combination with medium cohesion values was assigned to phyllites. For  $T/R$ , the standard values from SINMAP were used. The lowest cohesion and highest friction angle values were assigned to the class of sandstones and mudstones. Relatively low  $T/R$  values were chosen because a low permeability was assumed. The highest  $T/R$  and cohesion values were added to the limestones and slates which have been described as relatively compact and not affected by karst processes.

Table 3

Geotechnical parameter values for the classes of the Geological map (1:200000) for Youfang catchment

Class	Description	$C_{min}$	$C_{max}$	$\Phi_{min}$	$\Phi_{max}$	$T/R_{min}$	$T/R_{max}$
Phyllite	Mostly phyllites; some quartzites, sericite tuff, carbonaceous phyllite, slate, limestone, chert and fine siltstone	0	0.25	15	25	2,000	3,000
Sandstone/Mudstone	Mud-and-siltstone, silty mudstone and muddy siltstone and sandstone, conglomerates	0	0.2	25	35	1,000	2,000
Limestone/Slate	Thick layer of limestones and slates, some phyllites, chert, silty and fine sand	0	0.3	20	30	2,500	3,500

## 4.2. Modelling results

#### 4.2.1. Swabian Alb

Within the statistical analysis of SINMAP simulations, several features can be investigated. The most obvious aspect to analyse is the percentage of each stability class in the study area. Here, *no data* areas can be included or excluded. Similarly, the percentage of landslides in the stability classes can either be evaluated only for areas for which a stability index has been modelled, but also for *no data* areas. Finally, the degree to which the stability classes are affected by landslides can be quantified.

The susceptibility modelling with the 10 m data resulted in a very high proportion (56.3%) of the study area being classified as *stable* (Fig. 3A and Table 4). This class includes primarily the relatively flat areas of the plateau and some parts of the valley floor. The medium susceptibility classes *moderately-stable* and *quasi-stable* are present in the transition zone between *stable* areas and higher susceptibility classes. However, together they only make up approximately 11.7% of the study area. In steep and convergent slope sections, the *lower threshold* and the *upper threshold* are dominant. In total, 31.8% were classified with the respective stability classes. The proportion of areas classified as *defended* is very low (0.2%). This stability class is only present on some extremely steep sections of the limestone escarpment. When *no data* areas are included in the analysis, the respective numbers are slightly lower. In total, *no data* areas cover 7.6% of the study area.

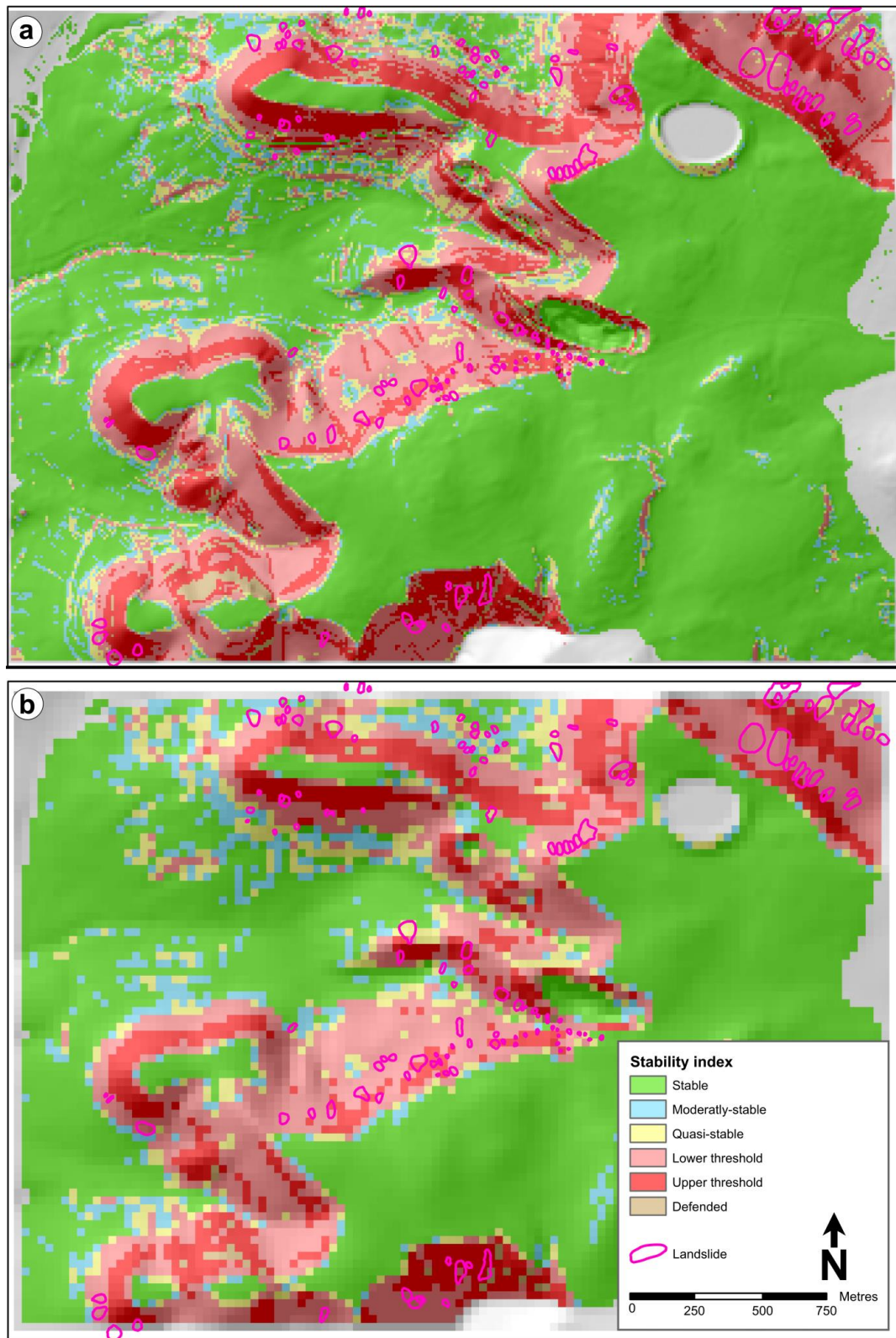


Fig. 3 – Landslide susceptibility maps for the study area in the Swabian Alb with (A) 10 m and (B) 30 m scale.

Table 4

Statistical summary of SINMAP modelling in the Swabian Alb study area

	10 m data set					30 m data set				
	Share of stability classes (in %)		Share of landslides (in %)		Share of stability classes affected by landslides (in %)	Share of stability classes (in %)		Share of landslides (in %)		Share of stability classes affected by landslides (in%)
	incl. <i>no data</i> area	excl. <i>no data</i> areas	incl. <i>no data</i> areas	excl. <i>no data</i> areas		incl. <i>no data</i> areas	excl. <i>no data</i> areas	incl. <i>no data</i> areas	excl. <i>no data</i> areas	
<b>Stable</b>	52.0	56.3	2.1	2.2	0.1	48.9	55.5	2.1	2.3	0.1
<b>Moderately-stable</b>	5.0	5.4	3.5	3.6	1.0	5.8	6.6	2.7	3.1	0.7
<b>Quasi-stable</b>	5.8	6.3	8.1	8.5	2.1	5.6	6.4	11.6	13.1	3.2
<b>Lower thresholds</b>	22.0	23.8	65.9	68.7	4.5	18.3	20.8	57.5	64.6	4.9
<b>Upper thresholds</b>	7.4	8.0	16.0	16.6	3.2	9.1	10.3	15.1	16.9	2.6
<b>Defended</b>	0.2	0.2	0.3	0.3	2.2	0.4	0.4	0.0	0.0	0.0
<b>No data</b>	7.6	–	4.0	–	0.8	11.9	–	11.0	–	1.4

The vast majority (85.3%) of landslide-affected areas are either in the *upper* or the *lower threshold* classes. In particular, the *lower-threshold* areas accommodate a large proportion of landslide-affected areas (65.9%). However, it is important to take into account that the entire landslide-affected area was used which, therefore, also includes run-out areas. However, the landslide initiation zones are often located within, or close to, areas classified as *upper threshold*. Relatively low proportions of landslide are located in the more stable stability classes. *Moderately-and-quasi-stable* areas include 3.6% and 8.5% of the landslide-affected areas, respectively, while *stable* areas account for only 2.2%. Again, the numbers are slightly different when *no data* areas are included in the analysis. A total of 4% of the landslide-affected areas are within such areas.

When the degree to which the respective stability classes are affected by landslides is analysed, the highest proportion can be found for *lower* and *upper-threshold* classes, with 4.5% and 3.2%, respectively. Only 0.1% of the areas modelled as *stable* are affected by landslides even though this stability class is by far the most abundant.

The SINMAP simulation using the 30 m input data resulted in a similar susceptibility map with a high proportion (55.5%) of *stable* areas in the relatively flat parts of the study area (Fig. 3B and Table 4). *Moderately-and-quasi-stable* areas account for approximately 6.5% each, and are again mainly located in the transition-zones between higher and lower stability classes. *Upper-and-lower threshold* areas are located on the steeper slope sections and account for 10.3% and 20.8% of the study area, respectively. Similar to the 10 m simulation, the proportion of defended areas is very low (0.4%). In comparison to the 10 m data set, the 30 m simulation includes a higher proportion of *no data* areas (11.9%). Overall, the 30 m susceptibility map shows a similar result as the 10 m map. However, the latter resembles a much finer classification. Topographic hollows and small-scale topography such as rivers or pathways are nicely highlighted by higher susceptibility classes, whereas the 30 m map does not distinguish these features because these are not well represented in the coarser data set. Additional differences can

be observed in the transition zones between *stable* areas and higher susceptibility classes; in the 10 m map, the lower threshold areas are often framed by *quasi-stable* and *moderately-stable* areas. This cannot be observed in the 30 m susceptibility map.

The comparison of landslide locations with susceptibility classification yielded similar results as for the 10 m simulation, with the largest proportion of landslides (81.5%) being located in the *upper-and-lower-threshold* areas. Again, the *lower-threshold* areas accommodate the largest share (64.6%) of landslide-affected areas. Classes of higher stability, i.e. *quasi-stable*, *moderately-stable* and *stable* have a relative low proportion of slope failures with 13.1%, 3.1% and 2.3%, respectively. These areas mostly include the run-out zones of the landslides, while the initiation zones are dominantly located in areas of lower stability, i.e. *lower* or *upper threshold*. When *no data* areas are also been taken into account, the share of landslides in each stability is slightly lower due to the fact that a total of 11% of all landslide-affected areas are within *no data* areas. The degree to which the stability classes are affected by landslides is very similar to the 10 m results.

#### 4.2.2. Youfang catchment

The results of SINMAP susceptibility modelling are presented in Fig. 4 and Table 5. In contrast to the study area in the Swabian Alb, the proportion of *no data* areas is larger (total of 28.4%), owing to the hydrological simulations in SINMAP and the poorer quality of the DTM available for Youfang. SINMAP's hydrological simulation step applies a flow routing algorithm. For the outmost pixels, as well as for grid cells for which no lower lying neighbour is available, the simulation cannot be carried out and the *no data* value is assigned. Similar to the previous simulations, the susceptibility map for Youfang dominantly shows lower stability classes for areas with steep slopes. However, since the topography in Youfang catchment is more extreme and fewer flat areas exist, the proportion of areas marked as *stable* is lower (14.1% if *no data* areas are excluded). *Moderately-stable* and *quasi-stable* areas account for approximately 4.5% and 10.1%, respectively. *Lower-threshold* areas cover approximately 43.3% and make up the largest part of the study area, and in particular large proportions of the slope areas. The *upper-threshold* class can primarily be found on the steepest slope sections and covers approximately 22.6%. Areas for which the calculated stability is always so low that stability cannot be calculated under the given parameter range (*defended*) can be found on several steep slopes and make up a total of 5.3% of the catchment. The percentage of the respective stability classes is about one third lower when *no data* areas are included in the analysis (see Table 5).

The three highest susceptibility classes in the Youfang study area, i.e. *defended*, *upper* and *lower threshold*, include approximately 67.5% of all the landslide-affected areas, and each class accounts for 2.5%, 17.7% and 47.3%, respectively. *Quasi-stable* areas contain 13.9% of the landslide-affected areas, and *moderately-stable* areas approximately 5.6%. The proportion of landslide-affected areas in the *stable* class is relatively high and totals approximately 12.9%. The previously mentioned percentages refer to the results in which *no data* areas were excluded. If these are taken into account, a total of 31.4% of the landslides are located in areas for which no stability index could be calculated. In comparison to the German study site, all stability classes of the Chinese study site are much more affected by landslides with percentages ranging between a minimum of 6.1% for the *defended* class and a maximum of 17.6% for the *quasi-stable* class. In particular the latter is surprising given that only a relatively few share of the study has been classified with this stability class.

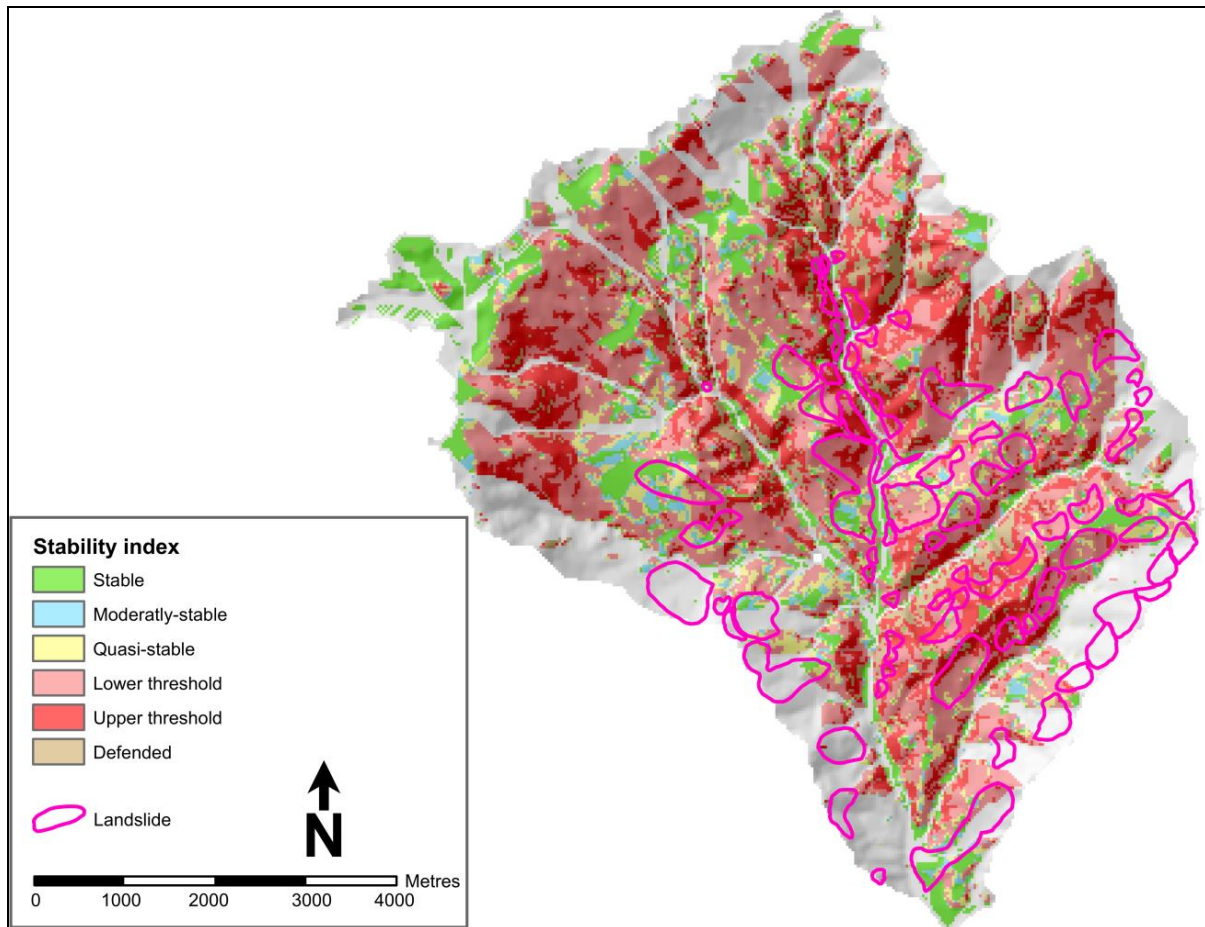


Fig. 4 – Landslide susceptibility map for the study area in Youfang study area with 30 m scale.

Table 5

Statistical summary of SINMAP modelling in the Wudu study area

	30 m data set				Share of stability classes affected by landslides (in %)
	Share of stability classes (in %)		Share of landslides (in %)		
	incl. no data areas	excl. no data areas	incl. no data areas	excl. no data areas	
<b>Stable</b>	10.1	14.1	8.9	12.9	11.8
<b>Moderately-stable</b>	3.2	4.5	3.9	5.6	16.0
<b>Quasi-stable</b>	7.2	10.1	9.5	13.9	17.6
<b>Lower thresholds</b>	31.0	43.3	32.4	47.3	14.0
<b>Upper thresholds</b>	16.2	22.6	12.2	17.7	10.1
<b>Defended</b>	3.8	5.3	1.7	2.5	6.1
<b>No data</b>	28.4	–	31.4	–	14.9

### 4.3. Sensitivity analysis

The results of the sensitivity analysis for the geotechnical parameters  $\Phi$ ,  $T/R$ ,  $C_{min}$  and  $C_{max}$  are presented in Fig. 5. A visual interpretation of the sensitivity plots highlights the differences of SINMAP susceptibility classification between the study areas in the Swabian Alb and Wudu county. In contrast to the Swabian Alb, the fraction of *stable*, *quasi-stable* and *moderately-stable* areas is much lower in the Youfang case study. Approximately 50% of the study areas are classified with the three lowest stability classes when the standard parameters are used. On average, the proportion of *defended*, *upper-and-lower-threshold* classes in Youfang is approximately 4%, 6% and 10% higher, respectively. However, the interpretation of the differences between the modelling results of both study areas has to take into account that the fraction of *no data* areas differs significantly, and is almost 17% higher for Youfang than for the Swabian Alb simulation using the same spatial resolution of input data. Still, the general influence of single parameters on susceptibility modelling can be assessed and compared.

The comparison of the results of the sensitivity analysis for the Swabian Alb using 10 m and 30 m input data show similar results and trends for the influence of geotechnical parameters. Tables 6 and 7 give a detailed overview on the changes between these two maps by highlighting the differences of the susceptibility classification between the 10 m and 30 m maps. An increased proportion of *no data* areas can be observed, which was 7.6% for the 10 m data and 11.9% for the 30 m data. Also the fractions of *defended* and *lower-threshold* areas tend to be larger for the coarser input data. Small changes in both directions have been observed for *quasi-stable* and *moderately-stable* stability classes. The proportion of *upper-threshold* areas generally decreased for all parameters except for the friction angle, while the fraction of *stable* areas decreased with coarser input data for all tested parameters.

When comparing the influence of the four geotechnical parameters on susceptibility modelling, substantial differences can be observed. In particular the modification of the internal friction parameter led to drastic changes of the proportions of susceptibility classes. The adjustment of the parameter values between 50% and 150% of the standard values changed the proportion of *stable* areas for approximately 40% for the data set from the Swabian Alb. Higher friction angle values also decreased the fraction of the two most unstable classes which both only account for less than 1% for the highest friction angle parameter values. In Youfang catchment, the largest changes can be observed for the *defended*-and *upper-threshold* classes, for which the fractions decrease by 27% and 20%, respectively, when the friction angle is raised from 50% to 150% of the standard parameter. In addition, the percentage of *stable* areas increased for approximately 38%. In contrast to the friction angle, the modification of the hydrological parameter  $T/R$  resulted only in small changes of the susceptibility classification for both study areas and for both input data resolutions. The modification of  $T/R$  parameter values in the range of 50% and 150% of the standard values resulted in relatively small changes of approximately 2% on average. The largest changes (8.6%) can be observed for *stable* areas using the 30 m data in the Swabian Alb. The modification of maximum cohesion only caused changes of the three highest susceptibility classes. In comparison to the friction angle, the changes of susceptibility classification due to a modification of  $C_{max}$  are relatively small and average 3.5%. The largest changes can be observed for the *lower-threshold* class up to a maximum of 15% in the Youfang study area. A modification of the  $C_{min}$  factor has a larger influence on susceptibility modelling in comparison to  $C_{max}$ . On average, a change of approximately 8% can be observed. Pronounced differences can be observed for the *lower-threshold* class where a high  $C_{min}$  value changed the respective fraction by up to 23%.

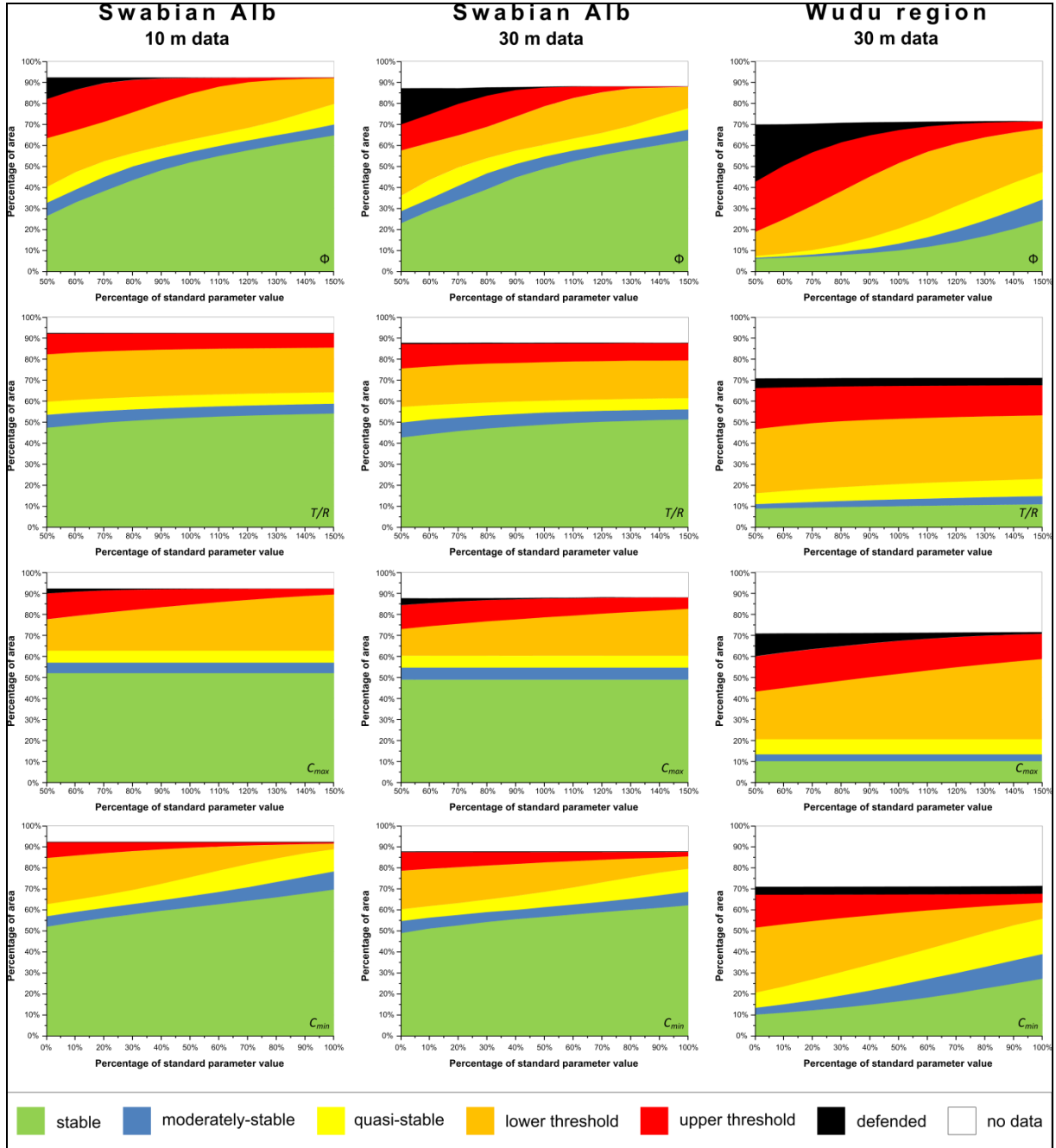


Fig. 5 – Sensitivity plots.

Table 6

Differences between the 10 m and 30 m sensitivity analysis for  $T/R$ , friction angle ( $\Phi$ ), and  $C_{max}$  for the Swabian Alb study area

		50%	60%	70%	80%	90%	100%	110%	120%	130%	140%	150%
<b>T/R</b>	no data	4.49	4.48	4.45	4.40	4.47	4.42	4.40	4.40	4.40	4.48	4.45
	stable	-4.40	-4.08	-3.76	-3.45	-3.27	-3.07	-2.83	-2.68	-2.64	-2.51	-2.59
	moderately-stable	0.97	1.13	0.94	0.86	0.83	0.82	0.55	0.44	0.37	0.14	0.12
	quasi-stable	1.24	0.70	0.52	0.25	0.15	-0.15	-0.13	-0.27	-0.24	-0.12	-0.11
	lower threshold	-4.42	-4.24	-3.95	-3.81	-3.90	-3.68	-3.54	-3.45	-3.33	-3.47	-3.40
	upper threshold	1.88	1.75	1.56	1.51	1.57	1.48	1.37	1.39	1.39	1.44	1.48
	defended	0.25	0.27	0.24	0.24	0.17	0.18	0.18	0.17	0.05	0.05	0.05
<b>PHI</b>	no data	5.20	5.13	5.18	4.75	4.63	4.42	4.23	4.29	4.27	4.28	4.27
	stable	-3.46	-3.99	-4.28	-4.40	-3.48	-3.07	-2.58	-2.25	-2.32	-2.42	-2.42
	moderately-stable	-0.54	-0.39	0.02	1.08	0.79	0.82	0.39	-0.13	-0.11	0.09	-0.03
	quasi-stable	-0.31	0.68	1.25	0.90	0.46	-0.15	-0.08	0.01	0.11	0.25	0.35
	lower threshold	-1.65	-2.34	-3.56	-4.62	-4.65	-3.68	-3.28	-2.52	-1.85	-2.27	-2.11
	upper threshold	-6.25	-5.74	-3.40	-0.49	1.36	1.48	1.27	0.64	-0.08	0.07	-0.06
	defended	7.01	6.65	4.78	2.77	0.89	0.18	0.06	-0.05	-0.03	-0.02	0.00
<b>C<sub>max</sub></b>	no data	4.63	4.70	4.60	4.59	4.54	4.42	4.39	4.17	4.21	4.23	4.27
	stable	-3.02	-3.07	-3.07	-3.07	-3.07	-3.07	-3.07	-3.07	-3.07	-3.07	-3.07
	moderately-stable	0.79	0.82	0.82	0.82	0.81	0.82	0.81	0.82	0.82	0.82	0.82
	quasi-stable	-0.18	-0.15	-0.15	-0.15	-0.19	-0.15	-0.15	-0.15	-0.15	-0.15	-0.15
	lower threshold	-2.26	-2.45	-2.80	-3.02	-3.40	-3.68	-4.04	-4.20	-4.39	-4.54	-4.46
	upper threshold	-1.01	-0.67	-0.13	0.41	0.95	1.48	1.89	2.26	2.50	2.68	2.59
	defended	1.06	0.83	0.73	0.43	0.36	0.18	0.18	0.18	0.08	0.04	0.00

Table 7

Differences between the 10 m and 30 m sensitivity analysis  $C_{min}$  for the Swabian Alb study area

		0%	10%	20%	30%	40%	50%	60%	70%	80%	90%	100%
<b>C<sub>min</sub></b>	no data	4.42	4.41	4.41	4.41	4.41	4.41	4.41	4.41	4.41	4.41	4.41
	stable	-3.07	-3.00	-3.54	-3.61	-3.99	-4.48	-4.88	-5.46	-6.01	-6.82	-7.54
	moderately-stable	0.82	0.34	0.27	-0.17	-0.55	-0.71	-1.09	-1.42	-1.92	-2.02	-2.07
	quasi-stable	-0.15	-0.34	-0.51	-0.79	-1.22	-1.76	-2.06	-1.75	-1.08	-0.35	0.32
	lower threshold	-3.68	-3.31	-2.87	-2.23	-1.16	0.08	1.20	1.93	2.56	2.87	3.32
	upper threshold	1.48	1.71	2.05	2.21	2.33	2.30	2.28	2.15	1.91	1.77	1.48
	defended	0.18	0.18	0.18	0.17	0.17	0.16	0.15	0.14	0.13	0.13	0.07

## 5. DISCUSSION

The application of SINMAP to the two study areas located in Germany and China resulted in generally reasonable susceptibility classification of the terrain, although the environmental and geomorphological conditions, and also data quality vary strongly between the two sites. Whereas the Swabian Alb study site features relatively shallow landslides and is covered by highly detailed topographic data, the Youfang catchment in China is affected by larger slope instabilities, also including rotational landslides, and is represented by a relatively poor DTM. Nevertheless, SINMAP produced acceptable susceptibility maps due to the physically-based methodology used; steep areas, topographic hollows and other areas of flow convergence, which are dominantly affected by shallow landsliding, feature lower stability classes. Still, due to the great differences between both studies, making a direct comparison between the model results is not feasible.

For the Swabian Alb, a relatively large area has been modelled as *stable*, and only a very small proportion of these areas are affected by landslides. In total, more than 80% of the landslide-affected areas are located in the three highest susceptibility classes when using the 10 m data set, and even with the coarser data these classes contained more than 72% of the landslide-affected areas. The *lower* thresholds stability class was hereby most affected by landslides but is also the second most common class in the simulations.

For Youfang, the proportion of high susceptibility classes is higher than in the Swabian Alb, and only 10% to 14% of the study area are modelled as *stable*, depending on the consideration of *no data* areas. It could be argued that these results represent an over-prediction of landslide susceptibility; however, the region is clearly an area of extreme landslide hazards, a fact that is also underlined by recent landslide events. A large proportion of landslide-affected pixels (46.3% - 67.5%) are located in areas that have been modelled as potentially unstable. The highest concentration of landslides was found in areas of relatively high stability, i.e. *moderately-stable* and *quasi-stable*, indicating a poorer stability classification. It should be noted, that the study in Youfang catchment was hampered by the lack of detailed topographic data. Digitising the only publicly available topographic map, and the subsequent transfer to a 30 m grid resulted in a low accuracy DTM which strongly affected the SINMAP simulations. It can be expected that the simulation results would greatly improve if better topographic data became available, preferably from LiDAR. Additional improvements of the model results could be achieved by extensive field and laboratory measurements of the constituents of the *T/R* factor, which in this study had to be based primarily on the subjective interpretation of limited geotechnical data.

In contrast to the majority of SINMAP applications, this study used the entire landslide-affected area for the quality assessment of SINMAP results instead of the point of landslide initiation. Consequently, there is a tendency of higher fractions of landslides being located in low susceptibility areas because the run-out zones may also affect flat areas, which are not likely to experience instability.

Inevitably, uncertainties remain in the application of a regional landslide simulation model. In this study, uncertainties arise from the methodology applied and the input data used. SINMAP is based on the infinite slope stability model which simplifies the real conditions of slope stability. Still, many case studies showed that that appropriate assessments of slope stability can be made in spite of the inherent simplifications. Topographic data represent the most important input for the SINMAP model and some shortcomings for the Youfang catchment data set have already been discussed. In addition, data on the spatial distribution of landslides were used to validate the results of SINMAP. For the Swabian Alb, it was possible to only include shallow slope failures which relied primarily based on DTM-based mapping. In contrast, because of the large extent of the Youfang catchment, as well as the remote location and the absence of high-detail DTM data, it was not possible to carry out mapping

campaigns similar to the Swabian Alb study site. Moreover, the 30 m pixel size made it impossible to detect or even represent small landslides from the topographic data. Moreover, due to the large size of many of the known slope failures in this region, it must be assumed that these are in many cases deep-seated and by definition not suited for SINMAP simulation. Another issue is the unknown age of the landslides, in particular in the Chinese study area where slope failures are larger and potentially very old. Arguably, one of the most important limitations of this study is the determination of geotechnical parameters which was significantly influenced by expert knowledge and subjective interpretation. To a certain extent, the uncertainties due to geotechnical parameter selection are accounted for by the integration of parameter ranges integrated into the SINMAP code and repeated modelling with SINMAP in order to calibrate the input parameters. Still, the  $T/R$  factor could not easily be determined because it is only used by SINMAP, and the information required deriving from it, for example, soil depth and information and landslide-triggering rainfall conditions, is not readily available and could only be assumed with great uncertainties. Using the assumed parameter values based on the SINMAP standard settings resulted in appropriate results, however, the sensitivity analysis revealed that under the used parameter range,  $T/R$  only has a very small influence on susceptibility modelling. From these results of this study, it cannot be concluded if the low influence of  $T/R$  is related to parameterisation, or to a general aspect of the SINMAP model.

Given these limitations, the presented work should be regarded as a basic estimation of the landslide susceptibility in the study areas. The resulting maps can be used to communicate the prevailing landslide susceptibility conditions and to highlight hot-spots of landslide susceptibility; however, such regional studies cannot replace more detailed site investigations.

## 6. CONCLUSIONS

This study presents the application of SINMAP to study areas with very different environmental and geomorphological conditions, data availability and sizes of study areas. A subsequent analysis of model sensitivity to geotechnical input parameters demonstrated a strongly varying influence of the involved parameters.

SINMAP allowed for a relatively quick computation of landslide susceptibility for large areas and generally assigned higher susceptibility classes to steep slope sections, and to areas where water flow convergence occurs. The results of this research show that a large proportion of the landslide-affected areas are located in areas for which high susceptibility was modelled. However, due to the limited availability of data, in particular the lack of high-detail topography data and verified geotechnical parameters of the critical soil layers involved in landsliding, this study can only represent a preliminary assessment of the regional landslide susceptibility. The simulation of landslide susceptibility with 10 m and 30 m input data in the Swabian Alb showed that both produced similar results despite the fact that small topographic features are not included in the coarser dataset. The most apparent differences could be observed in the transition zones between high and low susceptibility zones which are not well represented in the 30 m susceptibility map. The results suggest that 30 m input data can be used to derive appropriate susceptibility classifications when the size of the landslides is relatively large. Small landslides, close to the raster resolution and influenced by small scale topographical features, however, cannot be represented with this coarse base data. In contrast, the results of Youfang catchment had a lower quality with respect to the percentage of landslides being covered by highly susceptible areas, as well as the percentage of landslides within the high susceptibility classes. These poorer results for the Chinese study site can be attributed to the lack of more detailed topographic data, and highlight the benefits of LiDAR-based DTM for regional landslide analyses.

A sensitivity analysis of the geotechnical parameters was carried out to assess the influence of each parameter on the relative proportion of susceptibility classes. The results can be used by other researchers to calibrate the geotechnical parameters to achieve modelling results that better fit the distribution of slope failures in the respective study areas. According to the results, internal friction has the highest impact on the susceptibility simulation, while the  $T/R$  parameter only influences the model output to a small degree; however, this could also be related to the chosen parameter range and further tests including field measurements should be carried out.

### Acknowledgements

We would like to thank Horst Meyenfeld for providing the geotechnical database and Robert T. Pack, Research Associate Professor at Utah State University, USA, for his helpful comments on SINMAP. We are grateful towards the Landesanstalt für Umwelt, Messungen und Naturschutz (LUBW) for providing data for the Swabian Alb. Parts of this paper are based on research carried out within the InterRISK project which was funded by the German Research Foundation (DFG). Additional funding was granted by the 51<sup>st</sup> Chinese PostDoc Science Foundation (No. 2012M511298). We also like to thank the reviewers for their constructive comments.

### REFERENCES

- Aleotti, P. & Chowdhury, R. (1999), *Landslide hazard assessment, summary review and new perspectives*. Bulletin of Engineering Geology and the Environment **58** (1), pp. 21–44.
- Bai, S.B., Thiebes, B., Wang, J., Zhou, P.G. (2012), *Pre-conditioning factors for rainfall and earthquake-triggered landslides*. In: Eberhardt, E., Froese, C. R., Turner, A. K., and Leroueil, S., Edit. *Proceedings of the 11th International & 2nd North American Symposium on Landslides*. London, Taylor & Francis, pp. 501–505.
- Bai, S.B., Wang, J., Glade, T., Bell, R. (2010a), *Comparison of landslide susceptibility assessments before and after 5.12 Wenchuan Earthquake at Lognan in China*. In: Malet, J.-P., Glade, T., and Casagali, N., Edit. *Proceedings of the International Conference "Mountain Risks, Bringing Science to Society"*. Florence, Italy, pp. 87–94.
- Bai, S.B., Wang, J., Glade, T., Bell, R., Thiebes, B. (2010b), *Rainfall threshold analysis and landslide susceptibility mapping in Wudu county*. In: *Proceedings of the Second World Landslide Forum*. Rome, Italy.
- Bai, S.B., Wang, J., Lu, G.N., Zhou, P.G., Hou, S.S., Xu, S.N. (2009), *GIS-Based and Data-Driven Bivariate Landslide-Susceptibility Mapping in the Three Gorges Area, China*. Pedosphere **19** (1), pp. 14–20.
- Bai, S.B., Wang, J., Lü, G.N., Zhou, P.G., Hou, S.S., Xu, S.N. (2010c), *GIS-based logistic regression for landslide susceptibility mapping of the Zhongxian segment in the Three Gorges area, China*. Geomorphology **115** (1–2), pp. 23–31.
- Bell, R. (2007), *Lokale und regionale Gefahren- und Risikoanalyse gravitativer Massenbewegungen an der Schwäbischen Alb*. University of Bonn, Germany.
- Beven, K.J., Kirkby, M.J. (1979), *A physically based, variable contributing area model of basin hydrology*. Hydrological Sciences **24**, pp. 43–69.
- Bibus, E. (1986), *Die Rutschung am Hirschkopf bei Mössingen (Schwäbische Alb). Geowissenschaftliche Rahmenbedingungen – Geoökologische Folgen*. Geoökodynamik (7), pp. 333–360.
- Bibus, E. (1999), *Vorzeitige, rezente und potentielle Massenbewegungen in SW-Deutschland – Synthese des Tübinger Beitrags zum MABIS-Projekt*. In: Bibus, E. and Terhorst, B., Edit. *Angewandte Studien zu Massenbewegungen*. Tübinger Geowissenschaftliche Arbeiten. pp. 1–57.
- Bleich, K.E. (1960), *Das Alter des Albtraufs*. Jahreshefte des Vereins für Vaterländische Naturkunde in Württemberg **115**, pp. 39–92.
- Cascini, L. (2008), *Applicability of landslide susceptibility and hazard zoning at different scales*. Engineering Geology **102** (3–4), pp. 164–177.
- Catani, F., Casagli, N., Ermini, L., Righini, G., Menduni, G. (2005), *Landslide hazard and risk mapping at catchment scale in the Arno River basin*. Landslides **2** (4), pp. 329–342.
- Chen, Q.K. (2004), *The influence factor and distribution characteristic of geo-hazard in Wudu county*. Gansu Science and Technology **20** (9), pp. 139–141.
- Chen, W.W., Zhai, Z.F., Liu, G., Liang, S.Y. (2006), *The engineering geological problems of the Gansu section of Lanzhou-Haikou highway*. Lanzhou, Lanzhou University Press.
- China Geological Survey Bureau of Statistics (2008), *China Geological Environment InfoNet*. Retrieved at [www.cigem.gov.cn/defaulteng.html](http://www.cigem.gov.cn/defaulteng.html).

- Chung, C. (2008), *Predicting landslides for risk analysis – Spatial models tested by a cross-validation technique*. *Geomorphology* **94** (3–4), pp. 438–452.
- Cruden, D.M., Varnes, D.J. (1996), *Landslide types and processes*. In: Turner, A. K. and Schuster, R. L., Edit. *Landslides, Investigation and Mitigation (Special Report)*. Washington, D.C., USA, National Research Council, Transportation and Research Board Special Report **247**, pp. 36–75.
- Fell, R., Corominas, J., Bonnard, C., Cascini, L., Leroi, E., Savage, W.Z. (2008), *Guidelines for landslide susceptibility, hazard and risk zoning for land-use planning*. *Engineering Geology* **102** (3/4), pp. 85–98.
- Funding, A. (1985), *Ingenieurgeologische Untersuchung und geologische Kartierung (Dogger/Malm) der näheren Umgebung der Rutschungen am Hirschkopf bei Mössingen und am Irrenberg bei Thanheim (Baden-Württemberg)*. Geowissenschaftliche Fakultät, University Tübingen, Germany.
- Geyer, O., Gwinner, M.P. (1986), *Geologie von Baden-Württemberg*. Stuttgart, Germany, E. Schweizerbart.
- Guzzetti, F. (1999), *Landslide hazard evaluation, a review of current techniques and their application in a multi-scale study, Central Italy*. In: *Changing the face of earth, Engineering Geomorphology*, Proceedings of the 28th Binghamton Symposium in Geomorphology, held 28 August to 3 September 1997 in Bologna. p. 181.
- Guzzetti, F., Reichenbach, P., Cardinali, M., Galli, M., Ardizzone, F. (2005), *Probabilistic landslide hazard assessment at the basin scale*. *Geomorphology* **72** (1–4), pp. 272–299.
- Hammond, C., Hall, D., Miller, S., Swetik, P. (1992), *Level I stability analysis (LISA)*. U.S. Department of Agriculture, Forest Service, Intermountain Research Station.
- Kallinich, J. (1999), *Verbreitung, Alter und Ursachen von Massenverlagerungen an der Schwäbischen Alb auf der Grundlage von geomorphologischen Kartierungen*. In: Bibus, E. and Terhorst, B., Edit. *Angewandte Studien zu Massenbewegungen*. Tübinger Geowissenschaftliche Arbeiten. pp. 59–82.
- Krauter, E. (1992), *Hangrutschungen – ein Umweltproblem*. In: *Ingenieurvermessung '92*. XI. Internationaler Kurs für Ingenieurvermessung. Zürich, Switzerland, pp. 1–12.
- Kreja, R., Terhorst, B. (2005), *GIS-gestützte Ermittlung rutschungsgefährdeter Gebiete am Schönberger Kapf bei Öschingen (Schwäbische Alb)*. *Die Erde* **136** (4), pp. 395–412.
- Lan, H.X., Zhou, C.H., Wang, L.J., Zhang, H.Y., Li, R.H. (2004), *Landslide hazard spatial analysis and prediction using GIS in the Xiaojiang watershed, Yunnan, China*. *Engineering Geology* **76** (1–2), pp. 109–128.
- Legorreta Paulin: G., Bursik, M., Lugo-Hubp, J., Zamorano Orozco, J.J. (2010), *Effect of pixel size on cartographic representation of shallow and deep-seated landslide, and its collateral effects on the forecasting of landslides by SINMAP and Multiple Logistic Regression landslide models*. *Physics and Chemistry of the Earth, Parts A/B/C* **35** (3), pp. 137–148.
- Li, S.D. (1997), *Discussion on landslide activities in Bailong River basion of Wudu*. *Bulletin of Soil and Water Conservation* **17** (6), pp. 28–32.
- Meisina, C., Scarabelli, S. (2007), *A comparative analysis of terrain stability models for predicting shallow landslides in colluvial soils*. *Geomorphology* **87** (3), pp. 207–223.
- Meyenfeld, H. (2009), *Modellierungen seismisch ausgelöster gravitativer Massenbewegungen für die Schwäbische Alb und den Raum Bonn und Erstellen von Gefahrenhinweiskarten*. University of Bonn, Germany.
- Montgomery, D.R., Dietrich, W.E. (1994), *A physically based model for the Topographic control on shallow landsliding*. *Water Resources Research* **30** (4), pp. 1153–1171.
- Morrissey, M.M., Wiczorek, G.F., Morgan, B.A. (2001), *A Comparative Analysis of Hazard Models for Predicting Debris Flows in Madison County, Virginia*. USGS (ed.), Washington, D.C., USA, U.S. Department of the Interior, U.S. Geological Survey.
- Neuhäuser, B., Terhorst, B. (2007), *Landslide susceptibility assessment using “weights-of-evidence” applied to a study area at the Jurassic escarpment (SW-Germany)*. *Geomorphology* **86** (1–2), pp. 12–24.
- Ohmert, W., Von Koenigswald, W., Münzing, K., Villinger, E. (1988), *Geologische Karte 1:25.000 von Baden Württemberg*. Erläuterungen zu Blatt 7521 Reutlingen. Freiburg, Geologisches Landesamt Baden-Württemberg.
- Pack, R., Tarboton, D. (2004), *Stability Index Mapping (SINMAP) Applied to the Prediction of Shallow Translational Landsliding*. *Geophysical Research Abstracts* (6).
- Pack, R.T., Tarboton, D.G., Goodwin, C.N. (1998), *SINMAP - A stability index approach to terrain stability hazard mapping*. Retrieved from [http://digitalcommons.usu.edu/cgi/viewcontent.cgi?article=1015&context=cee\\_facpub](http://digitalcommons.usu.edu/cgi/viewcontent.cgi?article=1015&context=cee_facpub).
- Pack, R.T., Tarboton, D.G., Goodwin, C.N. (2001), *Assessing Terrain Stability in a GIS using SINMAP*. In: GIS 2001. 15th annual GIS conference. Vancouver, British Columbia, pp. 1–9.
- Pack, R.T., Tarboton, D.G., Goodwin, C.N., Prasad, A. (2005), *SINMAP 2 – A Stability Index Approach to Terrain Stability Hazard Mapping*. Retrieved at <http://www.engineering.usu.edu/dtarb/sinmap.html>
- Papathoma-Köhle, M., Neuhäuser, B., Ratzinger, K., Wenzel, H., Dominey-Howes, D. (2007), *Elements at risk as a framework for assessing the vulnerability of communities to landslides*. *Natural Hazards and Earth System Science* **7** (6), pp. 765–779.
- Petley, D. (2012), *Global patterns of loss of life from landslides*. *Geology* **40** (10), pp. 927–930.

- Schädel, K., Stober, I. (1988), *Rezente Großrutschungen an der Schwäbischen Alb*. Jahreshefte des Geologischen Landesamtes Baden-Württemberg (30), pp. 431–439.
- Scheidegger, A., Ai, N. (1987), *Clay slides and debris flows in the Wudu region*. Journal of Soil and Water Conservation 1 (2), pp. 19–27.
- Sidle, R.C., Wu, W. (1999), *Simulating effects of timber harvesting on the temporal and spatial distribution of shallow landslides*. Zeitschrift für Geomorphologie 43, pp. 15–201.
- Soeters, R., Van Westen, C.J. (1996), *Slope instability recognition, analysis, and zonation*. In: Turner, A. K. and Schuster, R. L., Edit. *Landslides, Investigation and Mitigation (Special Report)*. Washington, D.C., USA, National Research Council, Transportation and Research Board Special Report 247, pp. 129–177.
- Tarboton, D. (1997), *A new method for the determination of flow directions and upslope areas in grid digital elevation models*. Water Resources Research 33 (2), pp. 11.
- Tarolli, P., Tarboton, D.G. (2006), *A new method for determination of most likely landslide initiation points and the evaluation of digital terrain model scale in terrain stability mapping*. Hydrology and Earth System Sciences 10 (5), pp. 663–677.
- Terhorst, B. (1997), *Formenschatz, Alter und Ursachenkomplexe von Massenverlagerungen an der schwäbischen Juraschichtstufe unter besonderer Berücksichtigung von Boden- und Deckschichtenentwicklung*. Tübingen, Germany.
- Terhorst, B., Kreja, R. (2009), *Slope stability modelling with SINMAP in a settlement area of the Swabian Alb*. Landslides 6 (4), pp. 309–319.
- Thiebes, B. (2012), *Landslide analysis and early warning systems, Local and Regional Case Study in the Swabian Alb, Germany*. Springer.
- Thiebes, B., Bell, R., Glade, T. (2007), *Deterministische Analyse flachgründiger Hangrutschungen mit SINMAP – Fallstudie an der Schwäbischen Alb*. In: Kellerer-Pirklbauer, A., Keiler, M., Embleton-Hamann, C., & Stötter, J., Edit. *Geomorphology for the Future*. Innsbruck, Innsbruck University Press, pp. 177–184.
- Van Westen, C.J., Asch, T.W.J., Soeters, R. (2006), *Landslide hazard and risk zonation – why is it still so difficult?* Bulletin of Engineering Geology and the Environment 65 (2), pp. 167–184.
- Wagenplast, P. (2005), *Ingenieurgeologische Gefahren in Baden-Württemberg*. Freiburg, Germany, Landesamt für Geologie, Rohstoffe und Bergbau.
- Weerasinghe, K.M., Abeywickrema, H.V.M.P., Samarakoon, L., Fowze, J.S.M. (2007), *Use of a Deterministic Slope Stability Predicting Tool for Landslide Vulnerability Assessment in Ratnapura Area, Sri Lanka*. In: *Proceedings of the International Conference on Mitigation of Natural Disasters*. Peradeniya, Sri Lanka, pp. 1–17.
- Wu, W., Sidle, R.C. (1995), *A Distributed Slope Stability Model for Steep Forested Basins*. Water Resources Research 31 (8), pp. 2097–2110.
- Wu, W., Sidle, R.C. (1997), *Application of a distributed Shallow Landslide Analysis Model (dSLAM) to managed forested catchments in Oregon, USA*. In: *Human Impact on Erosion and Sedimentation*. Proceedings of the Rabat Symposium. IAHS Publication 245, pp. 213–222.
- Wu, W., Wang, N. (2006), *Landslide hazards in Gansu*. Lanzhou, Lanzhou University Press.
- Yin: Y. (2009), *Landslide mitigation strategy and implementation in China*. In: Sassa, K. & Canuti, P., Edit. *Landslides-Disaster Risk Reduction*. Berlin: Germany, Springer, pp. 482–484.
- Yu, B., Yang, Y.H., Su, Y.C., Wang, G.F. (2010), *Research on the giant debris flow hazards in Zhouqu county, Gansu Province on August 7, 2010*. Journal of Engineering Geology 18 (4), pp. 437–444.
- Zaitchik, B.F., Van Es, H.M. (2003), *Applying a GIS slope-stability model to site-specific landslide prevention in Honduras*. Journal of Soil and Water Conservation 58 (1), pp. 45–53.
- Zaitchik, B.F., Van Es, H.M., Sullivan, P.J. (2003), *Modeling slope stability in Honduras, Parameter sensitivity and scale of aggregation*. Soil Science Society of America Journal 67 (1), pp. 268–278.

Received September 10, 2015